ACS APPLIED MATERIALS & INTERFACES

Research Article

www.acsami.org

Effect of Hydrophobicity of Core on the Anticancer Efficiency of Micelles as Drug Delivery Carriers

Chun-Yang Sun,[‡,§] Yin-Chu Ma,[†,§] Zi-Yang Cao,[†] Dong-Dong Li,[†] Feng Fan,[†] Jun-Xia Wang,[†] Wei Tao,[†] and Xian-Zhu Yang*[,†]

[†]Department of Medical Materials and Rehabilitation Engineering, School of Medical Engineering, Hefei University of Technology, Hefei, Anhui 230009, China

[‡]School of Life Sciences and Medical Center, University of Science & Technology of China, Hefei, Anhui 230027, China

Supporting Information

ABSTRACT: Recently, micelles, which are self-assembled by amphiphilic copolymers, have attracted tremendous attention as promising drug delivery systems for cancer treatment. Thus, the hydrophobic core of the micelles, which could efficiently encapsulate small molecular drug, will play a significant role for the anticancer efficiency. Unfortunately, the effect of hydrophobicity of micellar core on its anticancer efficiency was rarely reported. Herein, the amphiphilic diblock polymers of poly(ethylene glycol) and polyphosphoester with different side groups (butyl, hexyl, octyl) were synthesized to tune the hydrophobicity of the micellar core. We found that the in vitro cytotoxicity of the DOX-loaded micelles decreased with the increasing hydrophobicity of micellar core due to the drug release rate. However, following systemic delivery, the DOX-loaded micelles with the most hydrophobic core exhibited the most significant inhibition of tumor growth in a MDA-MB-231 tumor model, indicating the importance of hydrophobicity of core on the antitumor efficacy of drug delivery systems.

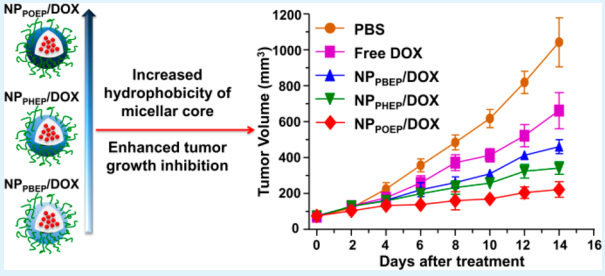

KEYWORDS: *polyphosphoester, hydrophobicity, micellar core, cancer therapy, drug delivery*

INTRODUCTION

Small molecular chemotherapeutic drugs are still one of the most common treatments for cancer, but its therapeutic efficacy is limited by the low bioavailability and side effects.[1−4] Over the past decades, self-assembled micelles based on amphiphilic block copolymers, which can efficiently encapsulate hydrophobic anticancer drugs,[5−10] have improved their pharmacokinetics and biodistribution profile and anticancer effect.[11−16] As an example, Samyang Corporation developed a micelles based on poly(ethylene glycol)-*block*-poly(lactide acid) (PEG-*b*-PLA) to encapsulate the paclitaxel, known as Genexol-PM, achieving 2−3-fold higher levels of biodistribution in tumors and is currently launched in the Korean market.[17] Among the current self-assembled micelles as drug delivery system, poly(ethylene oxide) (PEG) has been most widely used as the outer shell of micelles due to its superior capability to prevent plasma protein adhesion, and thus increase the circulation time of drug following intravenous injection.[18−21] On the other hand, biodegradable aliphatic polyesters, including poly(lactide acid) (PLA),[22] poly(d,l-lactide-*co*-glycolide) (PLGA),[23,24] poly(ε-caprolactone),[25] and poly(hydroxybutyrate),[26] are usually used as the hydrophobic core.[27] The hydrophobicity of these aliphatic polyesters contributes to the formation of the hydrophobic core of micelles.[28,29] Previous studies from Langer's group have demonstrated that the release rate of encapsulated drug depend on the composition of micellar hydrophobic core, which subsequently affect the antitumor efficacy.[30] Therefore, the hydrophobicity of the core could significantly closely relate to the antitumor efficacy of the drug-loaded micelles. To the best of our knowledge, the effect of hydrophobicity of the micellar core on the antitumor efficacy was rarely reported. Because tuning the hydrophobicity of the micellar core is difficult.

Polyphosphoesters (PPEs) with repeating phosphoester linkages in the backbone were a kind of biodegradable polymer for biomedical applications.[31] Up to now, lots of PPEs based polymers bearing different reactive pendant groups such as alkyl,[32] hydroxyl,[33] allyl,[34] and amino groups[35] have been developed. Recently, Wooley et al. have demonstrated that the PPEs could converted into hydrophobic polymers via introducing a relative bulky alkyl group.[32] The pentavalent nature of phosphorus in the backbone provides more structural flexibility of PPE polymers. Thus, its properties can be adjusted through changing the side group conjunct to phosphorus. It is possible to tune the hydrophobicity of the polyphosphoester by the side chains.

Herein, we synthesized three amphiphilic copolymers of PEG and PPE via the ring-opening polymerization of cyclic phosphoester monomers bearing different alkyl chain lengths. These amphiphilic block copolymers can self-assemble into core−shell

Received: October 6, 2014
Accepted: November 26, 2014
Published: November 26, 2014

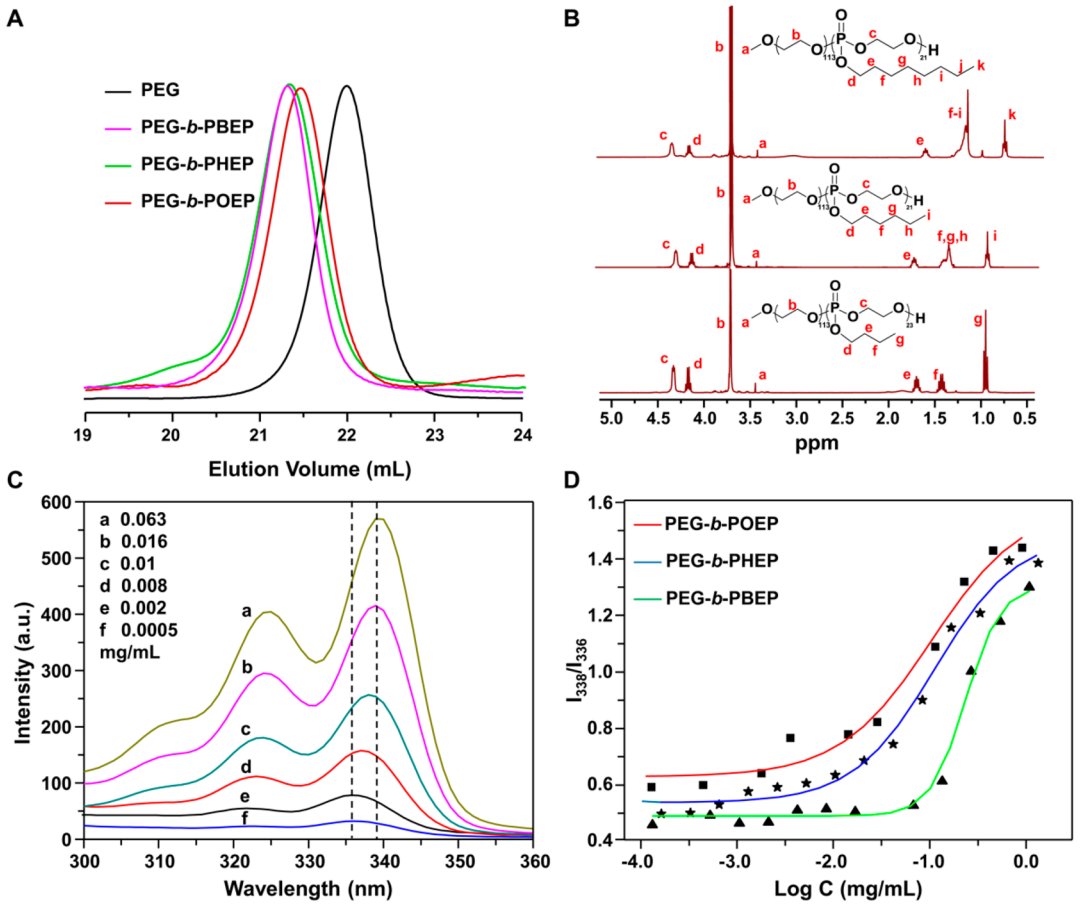

Figure 1. (A) GPC spectra of PEG, PEG-*b*-PBEP, PEG-*b*-PHEP, and PEG-*b*-POEP. (B) ^{1}H NMR spectra of PEG-*b*-PBEP, PEG-*b*-PHEP, and PEG-*b*-POEP (in $CDCl_3$). (C) Excitation spectra of pyrene in aqueous solution of PEG-*b*-PHEP at various concentrations (λ_{em} = 373 nm). (D) Plot of the I_{338}/I_{333} ratio (from pyrene excitation spectra) versus log C for PEG-*b*-PBEP, PEG-*b*-PHEP, and PEG-*b*-POEP.

micelles with a hydrophobic PPE core, which allows the hydrophobic DOX encapsulation. The influence of hydrophobicity of the core about cellular internalization, intracellular drug release, and in vitro cytotoxicity were observed. Also, the biodistribution, pharmacokinetics and therapeutic efficacy for MDA-MB-231 tumor following systemic administration were demonstrated to reveal how the hydrophobicity of the micellar core affects its anticancer efficiency.

EXPERIMENTAL SECTION

Materials and Characterizations. Pyrene, 1-butanol, 1-hexanol, and octanol were purchased from Aladdin Chemical Co., Ltd. (Shanghai, China). 2-Chloro-2-oxo-1,3,2-dioxaphospholane (COP) was synthesized by a method described previously,[36] then it was distilled under reduced pressure before use. Ultrapurified water (18 M Ω cm) was prepared using a Milli-Q synthesis system (Millipore, Bedford, MA). The hydrophobic drug DOX was obtained by incubating DOX·HCl (Zhejiang Hisun Pharmaceutical Co., Ltd., 10.0 mg) with triethylamine (Aladdin Chemical Co., Ltd., 3.5 mg) in dimethyl sulfoxide (DMSO) overnight. Dulbecco's modified eagle medium (DMEM) and fetal bovine serum (FBS) were purchased from Gibco and Hyclone, respectively. Monomethoxy PEG (M_n = 5000 g/mol), 3-(4,5-dimethylthiazol-2-yl)-2,5-diphenyl tetrazolium bromide (MTT), and 1,5,7-Triazabicylo[4.4.0]dec-5-ene (TBD) were purchased from Sigma−Aldrich.

The molecular weights and the molecular weight distributions were measured on a Waters gel permeation chromatography (GPC) system.[37] Nuclear magnetic resonance (NMR) spectra were recorded in deuterated chloroform ($CDCl_3$) or deuterated water (D_2O) with an AVANCE III 400 MHz NMR spectrometer. The size of the micelles and size change of micelles incubated with 10% FBS was measured in aqueous solution by Malvern Zetasizer Nano ZS90 dynamic light scattering instrument with a He−Ne laser (633 nm) and 90° collecting optics. The concentration of doxorubicin (DOX) was determined by high-performance liquid chromatography (HPLC) using a Waters 1525 HPLC system according to previously reported method.[38]

Synthesis of Cyclic Phosphoester Monomers. 2-Butoxy-2-oxo-1,3,2-dioxaphospholane (BEP), 2-hexoxy −2-oxo-1,3,2-dioxaphospholane (HEP) and 2-octoxy-2-oxo-1,3,2-dioxaphospholane (OEP) were synthesized by esterification of 2-chloro-2-oxo-1,3,2-dioxaphospholane (COP) with 1-butanol, 1-hexanol, and 1-octanol, respectively. Briefly, alcohol and triethylamine (TEA) were dissolved in anhydrous tetrahydrofuran (THF) at 0 °C. A solution of COP in anhydrous THF was dropwise added to the former mixture under magnetic stirring. The molar ratio of COP/TEA/alcohol was 1/1/1. The reaction was carried out at 0 °C overnight. After the reaction, the salt was removed first through a Schlenk funnel under N_2. The filtrate was concentrated and distilled under a vacuum to obtain the product.

Synthesis of Diblock Copolymer PEG and PPE. The diblock of PEG and PPE with different side group was obtained by ring-opening polymerization of different cyclic phosphoester monomers using PEG as the macroinitiator. The TBD was used as the catalyst.[39] In a typical example, PEG (0.500 g, 0.10 mmol, M_n = 5000 g/mol) and monomer (3.40 mmol) were mixed in anhydrous THF (9.1 mL) in a fresh flamed and nitrogen-purged flask. After stirring for 10 min, TBD (13.9 mg, 0.10 mmol) was added. The reaction was further stirred for 5 min, and then terminated with benzoic acid (0.122 g, 1.0 mmol). The residue was concentrated and precipitated into a cold diethyl ether/methanol mixture (10/1, v/v) twice.

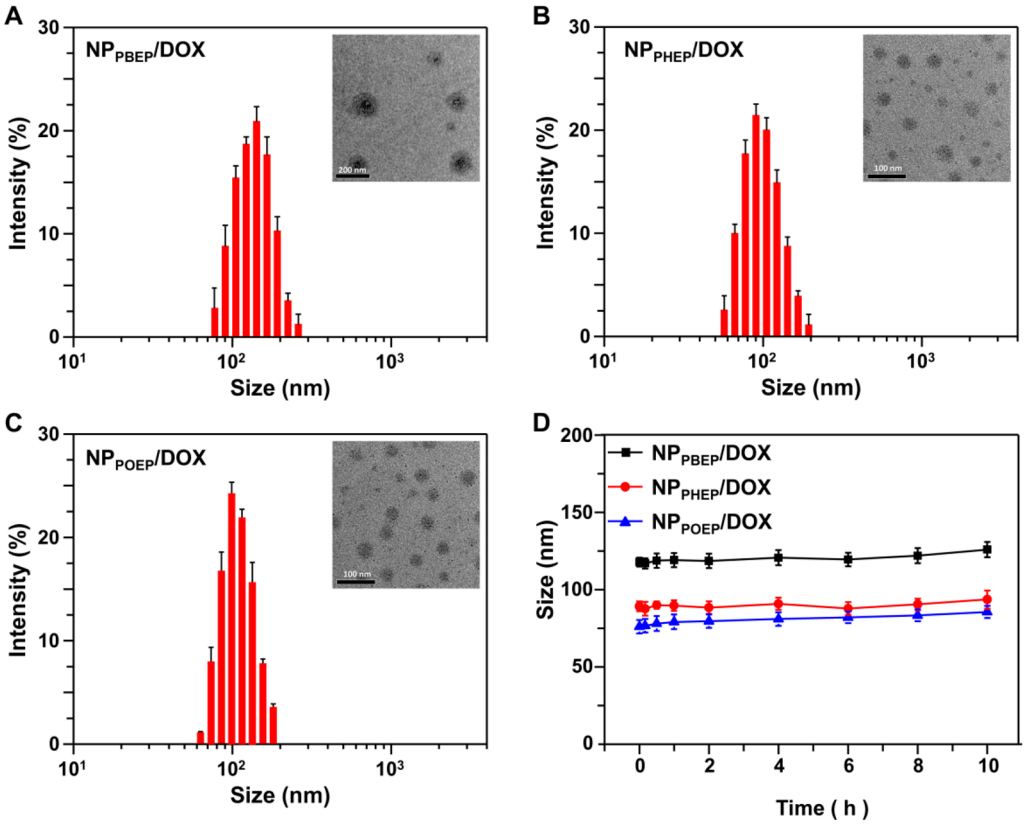

Figure 2. Dynamic light scattering measurement and transmission electron microscopic image of (A) NP_{PBEP}/DOX, (B) NP_{PHEP}/DOX, and (C) NP_{POEP}/DOX. (D) Changes in size of the micelles NP_{PBEP}/DOX, NP_{PHEP}/DOX, and NP_{POEP}/DOX in DMEM medium containing 10% FBS.

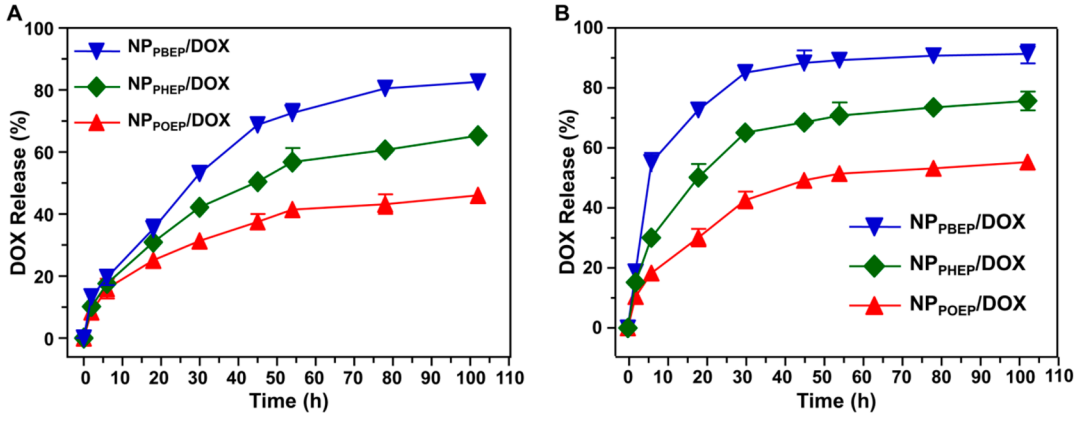

Figure 3. In vitro release of DOX from NP_{PBEP}/DOX, NP_{PHEP}/DOX, and $NP_{POEP/DOX}$ at different pH (A) 7.4 or (B) 5.5.

Critical Micellization Concentration (CMC) Measurements. To detect the CMCs of these amphiphilic diblock copolymers, we first prepared the micelles by the dialysis method. Typically, ultrapurified water (10 mL) was dropwise added to the DMSO solution of the diblock polymer (10 mg) through a syringe pump under gentle stirring. After stirring for an additional 3 h, the solution was transferred to a dialysis tube (MWCO 3500) to remove DMSO. After dialysis against ultrapure water for 24 h, the micelles were obtained. Subsequently the fluorescence probe pyrene was used to detect the CMC according to previously reported method.[40]

Preparation of DOX-Loaded Micelles. The DOX-loaded micelles of these copolymers were prepared through nanoprecipitation method. Typically, the 1.0 mL DMSO solution of diblock copolymers (10.0 mg) and DOX (1.0 mg) were dropwise added to 10 mL of ultrapurified water under stirring. After further stirring for 2 h, the solution was transferred to a dialysis tubing (MWCO 3500) and dialyzed against ultrapurified water for 24 h. The unloaded DOX was removed through a 0.45 μm filter (Millipore), and the DOX-loaded micelles were obtained.

In Vitro Drug Release. DOX-loaded micelles aqueous solution was suspended in phosphate buffer (PB buffer, 0.02 M, pH 7.4 or 5.5) at a DOX concentration of 50 μg/mL. The solution (1 mL) was transferred into the dialysis membrane tubing (MWCO 14 kDa). Then the tubing was immersed in the each buffer (10 mL) at 37 °C with gentle shaking (80 rpm). The external PB buffer was collected at predetermined intervals and lyophilized for HPLC analysis to determine the concentration of DOX.

Cell Culture. The human MDA-MB-231 breast cancer cells from the American Type Culture Collection (ATCC) were cultured in complete medium (DMEM with 10% FBS) at 37 °C in a 5% CO_2 atmosphere.

dx.doi.org/10.1021/am5068723 | ACS Appl. Mater. Interfaces 2014, 6, 22709−22718

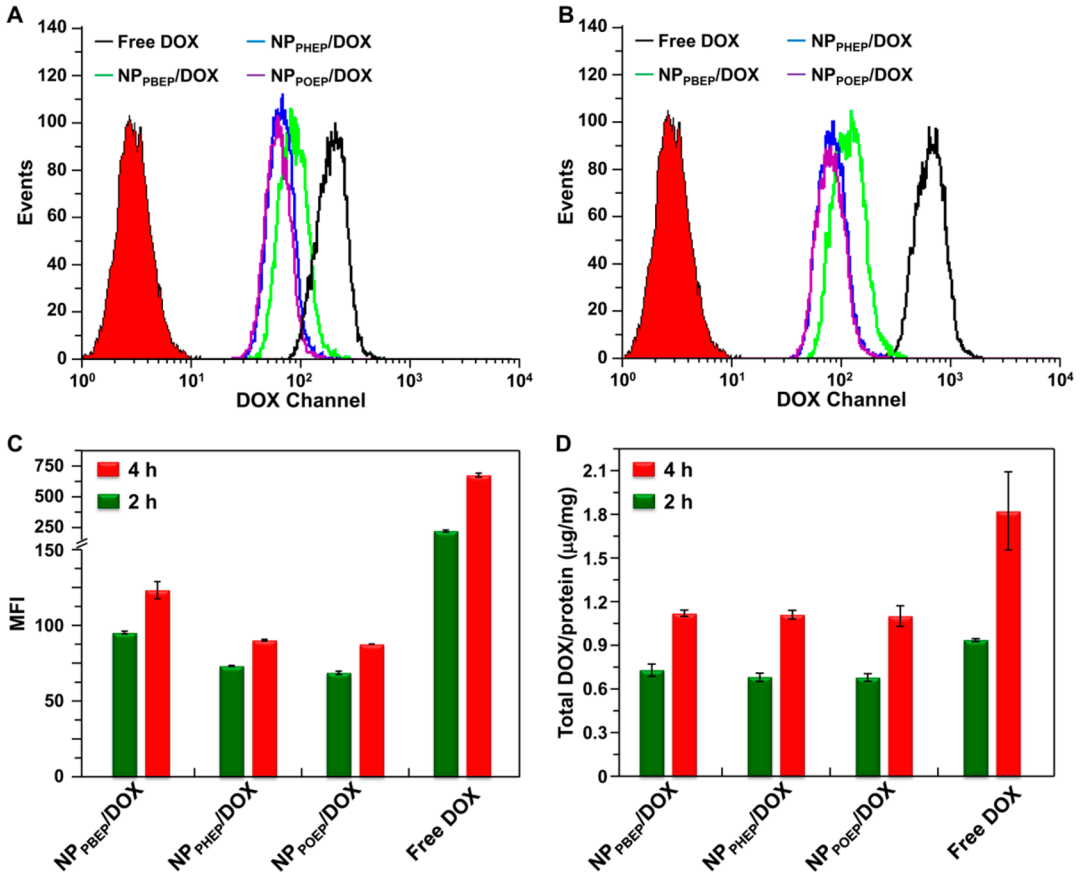

Figure 4. (A, B) Flow cytometric analyses of MDA-MB-231 cells after incubation with free DOX or DOX-loaded micelles (NP_{PBEP}/DOX, NP_{PHEP}/DOX, and NP_{POEP}/DOX) for (A) 2 or (B) 4 h. (C) Relative MFI from flow cytometric analyses for 2 and 4 h. (D) Total DOX accumulation in MDA-MB-231 cells after incubation for 2 and 4 h. The final concentration of DOX in the culture medium was 4.0 μg/mL.

Cell Internalization. For flow cytometric and HPLC analysis, MDA-MB-231 cells were seeded in 24-well plates (5×10^4 cells per well). After incubation at 37 °C with 5% CO_2 overnight, the medim was replaced with fresh complete DMEM medium. Then, free DOX or DOX-loaded micelles were added, and the final DOX concentration was 4.0 μg/mL in the culture medium. After further incubation for 2 or 4 h, the cells were washed with PBS, trypsinized, and fixed with 1% formaldehyde for FACS analyses (FACS Calibur flow cytometer, BD Biosciences, USA) and HPLC analyses according to a previously reported method.[41]

Additionally, to analyze the intracellular distribution, the MDA-MB-231 cells were seeded on coverslips in 24-well plates overnight. The medium was replaced fresh complete medium as descript above. After being incubated for 6, 12, or 24 h at 37 °C, the cells were washed with PBS, fixed with 1% formaldehyde, and counterstained with Alexa Fluor 488 phalloidin.

In Vitro Cytotoxicity Assays. MDA-MB-231 cells (5000 cells per well) were seeded in 96-well plates in DMEM (100 μL) and further incubated overnight. The original medium was replaced with fresh complete medium containing free DOX or DOX-loaded micelles at different DOX concentrations. After 72 h of incubation, MTT assay was used to analyze the cell viability according to the standard protocol.

Pharmacokinetics Studies. DOX or DOX-loaded micelles were intravenously injected into ICR mice at a DOX dose of 10 mg per kg weight (n = 4 for each group). The blood samples were collected at the predetermined time point. The blood was treated, and the concentration of DOX in the plasma was analyzed by HPLC as previously reported methods.[41]

Animals and Tumor Model. Female BALB/c nude mice (6 weeks old) purchased from the Beijing HFK Bioscience Co., Ltd. were used to establish a human breast cancer xenograft MDA-MB-231 tumor model and all animals received care in compliance with the guidelines outlined in the Guide for the Care and Use of Laboratory Animals. The procedures were approved by the University of Science and Technology of China Animal Care and Use Committee. The cells (2×10^6 for each mouse) were injected into the mammary fat pat of female Balb/c nude mice. After the tumor volume reached 60 mm^3, the mice were used for subsequent experiments.

Drug Biodistribution. DOX or DOX-loaded micelles were intravenously injected into BALB/c nude mice bearing MDA-MB-231 xenograft tumors. The injection dose of DOX was 10 mg per kg weight (n=4 for each group). For imaging experiment, the mice were anaesthetized and imaged with a Xenogen IVIS Lumina system (Caliper Life Sciences, USA) at a predetermined time point. For quantitative analysis, the mice were sacrificed, and then the organs were collected, washed with PBS. Subsequently the DOX biodistribution was analyzed according to previously reported methods.[42] Moreover, the excised tumor tissues were fixed in 4% formaldehyde and then treated with 30% sucrose overnight. Five μm of tumor frozen sections were obtained, and counterstained with Alexa Fluor 488 phalloidinand with DAPI, respectively. Finally, the slices were observed by LCSM.

Inhibition of Tumor Growth. Balb/c nude mice bearing MDA-MB-231 xenograft tumors were randomly divided into five groups (n = 5), the above formulations were intravenously injected once every other days at an equivalent DOX dose of 5.0 mg/kg. The volume of the tumor was monitored every other day, and the estimated volume was calculated according to the formula: tumor volume (mm^3) = 0.5 × length × width^2.

Immunohistochemical Analysis. One day after the last injection, tumor tissues were excised, fixed in 4% formaldehyde, and embedded in paraffin for analysis. Paraffin-embedded 5 μm tumor sections were obtained for immunnohistochemical staining of the proliferating cell

nuclear antigen (PCNA) and the terminal transferase dUTP nick-end labeling (TUNEL) assay.[43]

RESULTS AND DISCUSSION

Synthesis of Amphiphilic Diblock Polymer of PEG and PPE with Different Side Groups. To demonstrate the effect of hydrophobicity of micellar core on anticancer efficiency of drug-loaded micelles, we synthesized the amphiphilic diblock polymers of PEG and PPE with different side groups to tune the hydrophobicity of the micellar core. First, we synthesized several of cyclic phosphoester monomers with different alkyl side groups, and obtained the corresponding diblock copolymer using PEG as macroinitiator. The polymerizations were accomplished rapidly to high monomer conversion in 5 min by TBD catalyzed ring-opening polymerization. Successful syntheses were confirmed by GPC and NMR analyses. As shown in Figure 1A, the elution volumes of these amphiphilic diblock polymers were all about 21.3 mL, against 22.20 mL of PEG. Compared with the macroinitiator PEG, the decrease of elution volume suggested the formation of diblock polymer. The ^{1}H NMR spectra of diblock polymers were depicted in Figure 1B, it was found that all the resonances could be assigned to the corresponding protons. The average degrees of polymerization (DP) of phosphoester block were calculated by comparisons of the integrals of proton resonances of PEG backbone (4.35 ppm) to those of PPE backbone(3.65 ppm), which indicated that the DP of these three diblock polymers PEG-*b*-PBEP, PEG-*b*-PHEP and PEG-*b*-POEP were 23, 21, and 21, respectively.

Self-Assembly of Amphiphilic Diblock Polymer of PEG and PPE with Different Side Groups and DOX Loading. To demonstrate whether the hydrophobicity of these synthesized polymers can be turned by the side group of PPE block, we analyzed the CMCs of these polymers by the fluorescent probe pyrene. As shown in Figure 1C, a red shift of the fluorescence excitation spectra of pyrene was observed with the increased concentration of diblock polymer, which indicated micelles were the prepared. The intensity ratios of the band at 338.0 and 336.0 nm from the excitation spectra were plotted against copolymer concentrations as shown in Figure 1D. From the sigmoidal shape curve, the CMC values were calculated as 1.2×10^{-1}, 6.3×10^{-2} and 5.2×10^{-3} mg/mL of PEG-*b*-PBEP, PEG-*b*-PHEP and PEG-*b*-POEP, respectively. The longer alkyl side groups will lead to increased hydrophobicity, resulting in stronger hydrophobic−hydrophobic interaction and lower CMC. These data demonstrated that these three diblock polymers (PEG-*b*-PBEP, PEG-*b*-PHEP and PEG-*b*-POEP) can form micelles with hydrophobic polyphosphoester core, and the hydrophobicity of core can be tuned by changing the side groups of PPE block. To further certify this speculation, these micelles were lyophilized, and the ^{1}H NMR spectra of these micelles in D_2O were analyzed. As shown in Figure S1 in the Supporting Information, the signals (δ 4.34) assigned to protons of PPE main chain gradually disappeared when the alkyl length of the side groups were increased, while signals of PEG block (3.72 ppm) were still prominent, indicating the hydrophobicity of hydrophobic polyphosphoester core increased with increasing alkyl length of the side groups.

To demonstrate the effect of hydrophobicity of micellar core on anticancer efficiency, we used DOX, which is one of the most commonly used chemotherapeutic drugs in clinic, as a model anticancer drug. After DOX loading, these three diblock polymers, PEG-*b*-PBEP-, PEG-*b*-PHEP-, and PEG-*b*-POEP-based micelles were denoted as $NP_{PBEP/DOX}$, $NP_{PHEP/DOX}$ and $NP_{POEP/DOX}$. As shown in Figure 2, the average sizes of these three DOX-loaded micelles were around 100 nm. The size of $NP_{PBEP/DOX}$ was slightly larger than $NP_{PHEP/DOX}$ and $NP_{POEP/DOX}$. TEM images showed the micelles took on a classic circular micelle structure with a slightly smaller average diameter compared with DLS measurements, indicating the existence of hydrophilic PEG corona in aqueous solution.

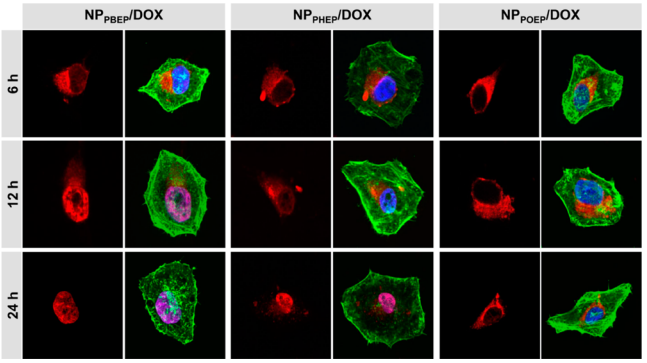

Figure 5. Cellular subcellular distribution of DOX-loaded micelles (NP_{PBEP}/DOX, NP_{PHEP}/DOX, and NP_{POEP}/DOX) for different periods of time.

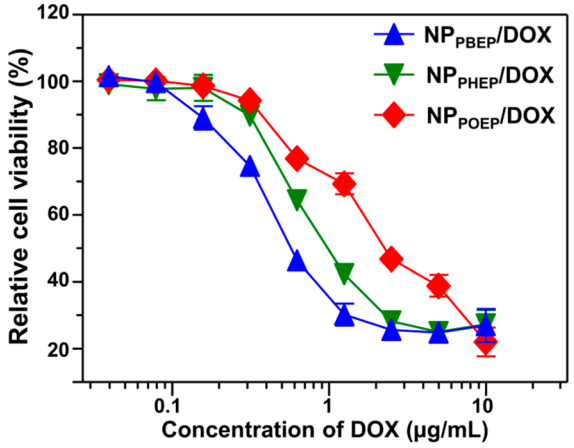

Figure 6. Cytotoxicity of DOX-loaded micelles (NP_{PBEP}/DOX, NP_{PHEP}/DOX, and NP_{POEP}/DOX) in MDA-MB-231 cells for 72 h.

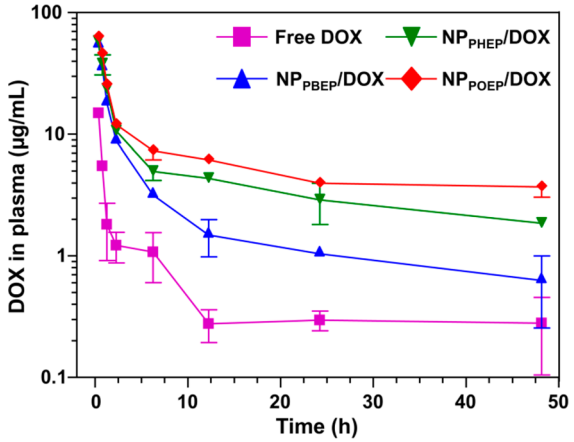

Figure 7. Plasma DOX concentration versus time after intravenous injection of free DOX or DOX-loaded micelles ($NP_{PBEP/DOX}$, $NP_{PHEP/DOX}$, and $NP_{POEP/DOX}$) (mean ± SD, n = 4).

dx.doi.org/10.1021/am5068723 | ACS Appl. Mater. Interfaces 2014, 6, 22709−22718

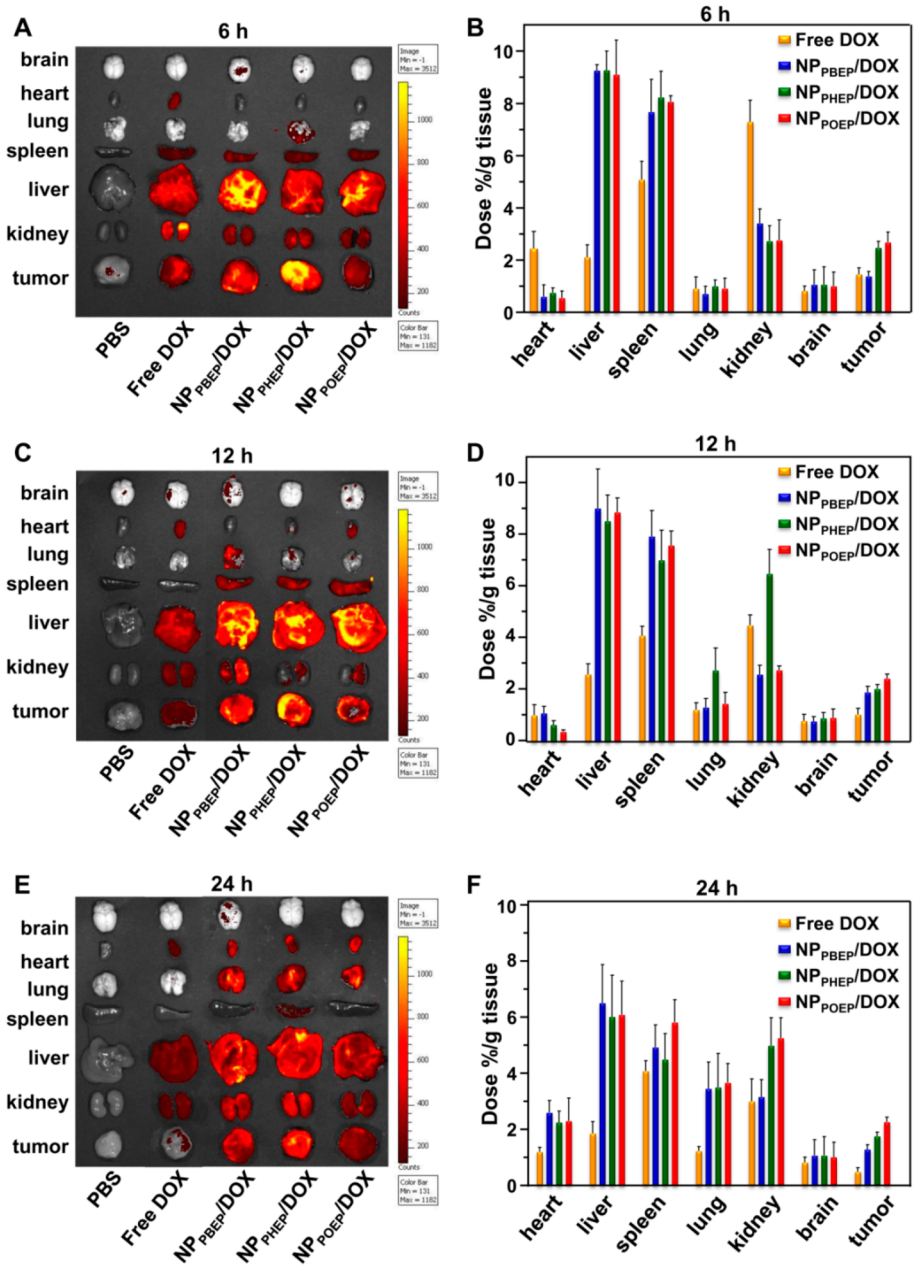

Figure 8. Fluorescence images and quantitative analyses of DOX content of main organs after administration of different formulations at (A, B) 6, (C, D) 12, and (E, F) 24 h (mean ± SD, n = 4). The dose of DOX was 200 μg per mouse.

Moreover, the PEG shell prevented aggregation of these micelles (Figure 2D).

The effect of hydrophobicity of micellar core on the drug release rate was first evaluated at pH 7.4 and pH 5.5. As shown in Figure 3A, the drug release rate from $NP_{POEP/DOX}$ was significantly decelerated compared with $NP_{PBEP/DOX}$ and $NP_{PHEP/DOX}$. Moreover, a similar trend was observed when the DOX-loaded micelles were incubated in buffer at pH 5.5 (Figure 3B). It should be noted that the glass transition temperature (Tg) for PEG-*b*-PBEP, PEG-*b*-PHEP and PEG-*b*-POEP were between −60 °C and −80 °C (see Figure S2 in the Supporting Information). Thus, the polymers were viscous flow state at room temperature, indicating that the state of the micellar core did not affect the drug release. Moreover, the drug release rate from hydrophobic polyphosphoester core was not affected by the degradation rate of the polymeric carriers.[44] These results indicated that the drug release rate was mainly depended on the hydrophobicity of the polyphosphoester core in these systems, and the drug release rate decreased with increasing hydrophobicity of micellar core.

Cellular Internalization and Intracellular Drug Distribution. We evaluated the cellular internalization of these DOX-loaded micelles by flow cytometry and HPLC. After incubation at 37 °C for 2 or 4 h, intracellular fluorescence was analyzed. As shown in Figure 4A−C, cells incubated with $NP_{PBEP/DOX}$ exhibited slightly stronger intracellular fluorescence than that incubated with $NP_{PHEP/DOX}$ or $NP_{POEP/DOX}$. This result could be because that the release rate of DOX from $NP_{PBEP/DOX}$, which was quenched after encapsulation (see Figure S3 in the Supporting Information), was faster than that from $NP_{PHEP/DOX}$ or $NP_{POEP/DOX}$ (Figure 3), which resulted in the enhanced intracellular fluorescence. The cellular internalization

was further quantitatively analyzed the concentration of DOX by HPLC (Figure 4D). According to the HPLC results, it was clearly demonstrated that cells cultured with these three DOX-loaded micelles had similar intracellular DOX contents, indicating that the hydrophobicity of micellar core did not influence the cellular uptake of these DOX-loaded micelles.

Followed by the FACS and HPLC detection, we demonstrated whether the hydrophobicity of the micellar core affected the intracellular DOX distribution by LCSM. As same as the FACS experiment, we incubated the MDA-MB-231 cells with DOX-loaded micelles for 2 h. And then the culture medium was replaced with fresh medium, and further incubated for 4, 10, or 22 h to avoid the extracellular released DOX. Alexa Fluor 488 phalloidin and DAPI were used to counterstain the cytoskeleton F-actin and cell nuclei, respectively. As displayed in Figure 5, the red fluorescence from $NP_{PBEP/DOX}$, $NP_{PHEP/DOX}$, or $NP_{POEP/DOX}$ was dominantly localized in cytoplasm at 6 h. However, after increased the incubation times, the red DOX fluorescence was gradually transferred from cytoplasm to nucleus when the cells were incubated with $NP_{PBEP/DOX}$, and there is merely signal outside the nucleus at 12 h. In contrast, after 12 h of incubation, most of the DOX were still retained in in the cytoplasm for $NP_{PHEP/DOX}$ and $NP_{POEP/DOX}$ groups. For $NP_{POEP/DOX}$ with the most hydrophobic core, DOX was rarely observed in the nuclei even after 24 h of incubation. This result indicated that the intracellular drug release rate decreased with increasing hydrophobicity of the micellar core. This phenomenon was consistent with the release profile of DOX from these micelles with different degrees of hydrophobic core (Figure 3).

In Vitro Cytotoxicity Assay of DOX-Loaded Micelles. DOX disturbed the tumor cells through the inhibition of replication, transcription and translation of DNA.[45] We have demonstrated the intracellular drug release and distribution could be affected by the hydrophobicity of micellar core. Furthermore, we incubated tumor cells with these DOX-loaded micelles for 72 h followed by a standard MTT assay to evaluate the cytotoxicity of these nanoparticles. As shown in Figure 6, $NP_{PBEP/DOX}$ exhibited the strongest cell growth inhibition, within an IC_{50} of 0.85 μg/mL, and the highest IC_{50} was 2.70 μg/mL for $NP_{POEP/DOX}$. These data demonstrated that although the hydrophobicity of micellar core did not influence the cellular uptake of these DOX-loaded nanoparticles (Figure 4), it significantly influence the in vitro cytotoxicity. $NP_{PBEP/DOX}$ with the weakest hydrophobic core was much more efficient in inhibiting cell growth.

Plasma Pharmacokinetics and Biodistribution. The tumor environment is highly complex, which could not be simulated simply in vitro. The effect of hydrophobicity of micellar core on its in vivo fate was further evaluated. The pharmacokinetics and biodistribution of these DOX-loaded micelles were first examined. These DOX-loaded micelles were intravenous injected into the ICR mice, and free DOX was used as control. The blood was collected at 5 min, 30 min, 1 h, 2 h, 6 h, 12 h, 24 h, and 48 h later, and the plasma DOX concentration was determined by HPLC. As shown in Figure 7, free DOX was eliminated rapidly after the intravenous injection. Among DOX-loaded micelles, the $NP_{PBEP/DOX}$ showed a relatively fastest clearance, which might be attributed to the fastest drug release rate (Figure 3) and the rapid clearance of released DOX. In contrast, prolonged half-time in blood circulation was observed for $NP_{PHEP/DOX}$ or $NP_{POEP/DOX}$. Meanwhile, the area under the concentration curve (AUC_{0-t}) of $NP_{PHEP/DOX}$ (225.65 ± 24.48 mg/(L h)) was lower than that of $NPP_{OEP/DOX}$ (309.53 ± 23.07 mg/(L h)), which analyzed by DAS 3.0 software. It is worth noting that the significant difference of the concentration of DOX between $NP_{PHEP/DOX}$ and $NP_{POEP/DOX}$ wasobserved only after a time point of 6 h. This result indicated that the micelles with the most hydrophobic core exhibited the longest circulation time, whereas $NP_{PEBP/DOX}$ with the weakest hydrophobic core was cleared rapidly from the circulation.

Furthermore, to demonstrate the effect of hydrophobicity of micellar core on drug biodistribution in vivo, we evaluated the DOX content in tumors following intravenous injection of above formulations into nude mice bearing MDA-MB-231 tumor model. The distribution was analyzed at different time point through the fluorescence signal collected by Xenogen IVIS Lumina system and HPLC quantitative detection. As shown in Figure 8A, free DOX was mainly cleared through kidney during first 6 h, and uptake by tumors was 1.46, 1.07, and 0.49% at 6, 12, and 24 h (Figure 8), respectively. In contrast, the tumor uptake of DOX was all enhanced for these three DOX-loaded micelles, and these micelles were primarily retained in the liver and spleen. Among these DOX-loaded micelles, the $NP_{PBEP/DOX}$ showed a lowest accumulation in tumor. For the other two groups, 2.45 and 2.07% of the injection dose per gram of tumor was detected for $NP_{POEP/DOX}$ at 6 and 12 h, whereas the $NP_{PHEP/DOX}$ only delivered 2.05 and 1.68% of the injection dose to pre gram of tumor ($p < 0.05$). Therefore, we speculate that although the $NP_{POEP/DOX}$ exhibited the similar cellular uptake potencies to $NP_{PBEP/DOX}$ and $NP_{PHEP/DOX}$ (Figure 4), but it could avoid drug leak in the circulation because of the most hydrophobic core (Figure 7), resulting in the highest drug accumulation.

In addition, the cellular internalization of these formulations following intravenous injection was demonstrated by the confocal microscopic observations of tumor tissue sections (Figure 9). The strongest red fluorescent signal of DOX in

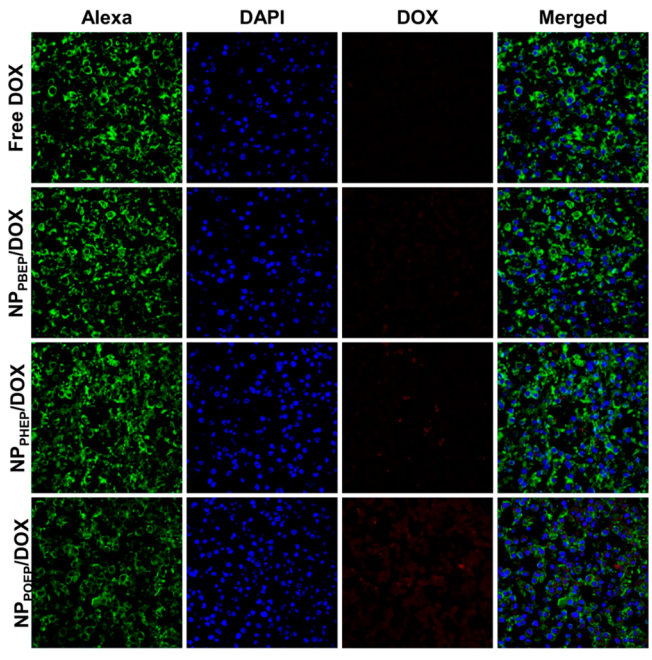

Figure 9. Free DOX, NP_{PBEP}/DOX, NP_{PHEP}/DOX, and NP_{POEP}/DOX internalized by tumor cell at 48 h after intravenous injection and the image were observed by LSCM. Cell nucleus and cytoskeleton were stained by Alexa Fluor 488 phalloidin (green) and DAPI (blue), respectively.

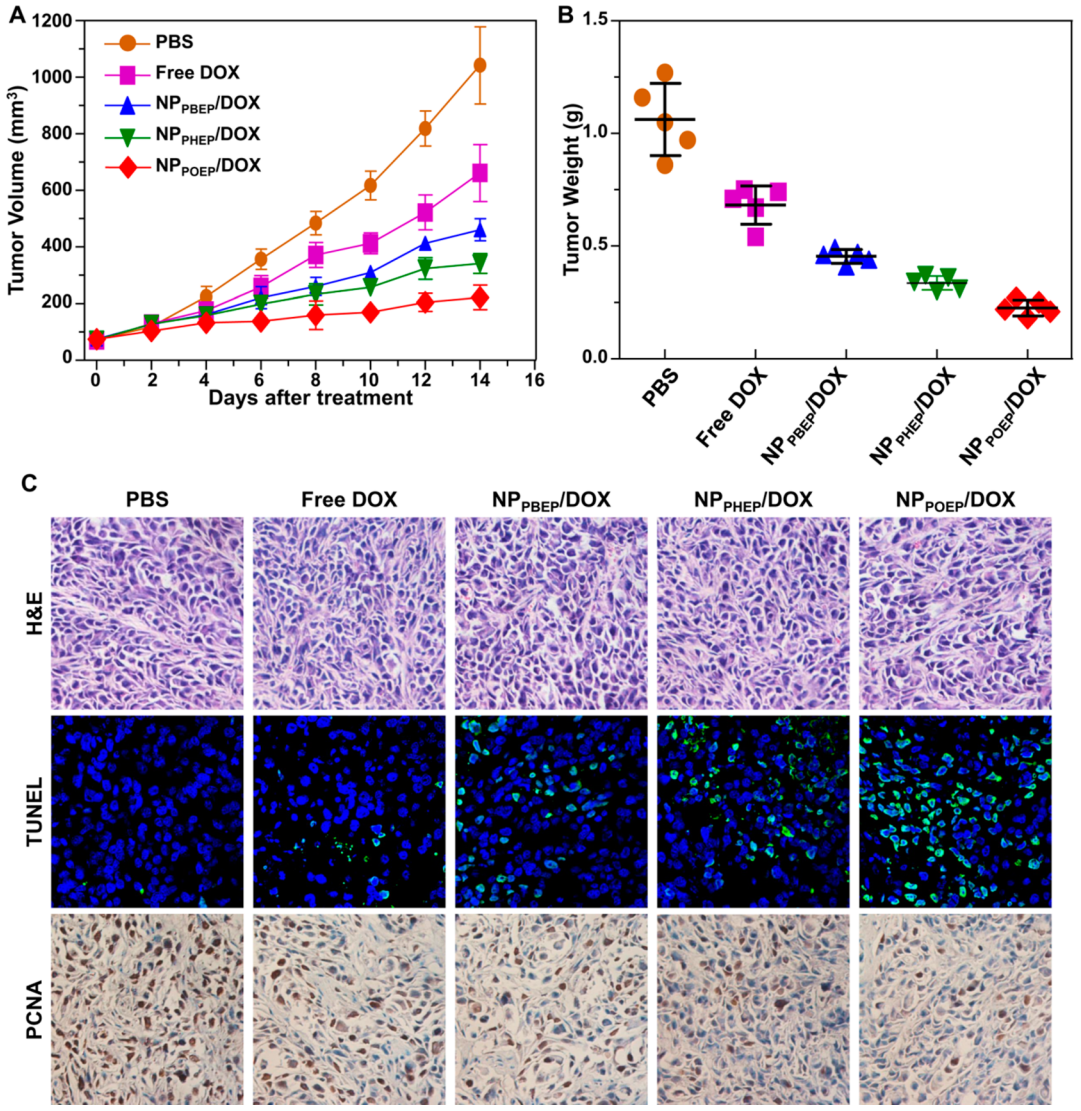

Figure 10. (A) Antitumor growth experiment of free DOX, NP_{PBEP}/DOX, NP_{PHEP}/DOX, and NP_{POEP}/DOX to MDA-MB-231-bearing nude mice (n = 5). (B) Tumor weight at the end point of the treatment; (C) hematoxylin-eosin staining, cell proliferation, and apoptosis in tumor tissue after the treatment.

tumor was observed following $NP_{POEP/DOX}$ administration, which confirmed that the highest drug accumulation in tumor tissue was due to the most hydrophobic core.

In Vivo Antitumor Efficacy. To evaluate the anticancer efficacies of these three DOX-loaded micelles, we establish MDA-MB-231 breast tumors in situ in Balb/c nude mice. After the average tumor volume exceeded 60 mm^3, mice were randomly divided into 5 groups and treated with PBS, free DOX (5.0 mg/kg) and DOX-loaded micelles at equivalent dose of DOX twice in 1 week. The tumor growth was moderately inhibited by intravenous injection of free DOX at 5.0 mg/kg compared with PBS group (Figure 10A). In contrast, all of the DOX-loaded micelles could inhibit the tumor growth more effectively compared with DOX groups. Among these three groups, the $NP_{PBEP/DOX}$ showed the lowest inhibition, whereas the $NP_{POEP/DOX}$ showed the best tumor inhibition. The tumor weight was also shown in Figure 10B, further supported the above result. Moreover, it is worth noting that the repeatedly injection of these formulations did not induce the change of body weight during the treatment (see Figure S4 in the Supporting Information), indicating that the antitumor efficacy of these formulations was not due to the cytotoxicity. These results demonstrated that the micelles with the most hydrophobic core were much more efficient in inhibiting tumor growth, which is significantly different compared with that in vitro.

Furthermore, we examined the cell proliferation (PCNA-positive) and apoptosis (TUNEL-positive) in tumor tissues after the treatment through immunohistochemical or immunofluorescence analyses. From Figure 10C, compared with PBS group, the free doxorubicin could increase cell apoptosis and reduce cell proliferation simultaneously. Corresponding to the tumor inhibition results, the administration of DOX-loaded micelles could markedly enhance the above effects, and the most obvious inhibiting proliferation and inducing apoptosis were found in $NP_{POEP/DOX}$ group.

CONCLUSIONS

In conclusion, to evaluate the effect of the hydrophobicity of micellar core on antitumor efficacy, we have rationally designed hydrophobic polyphosphoester-based micelles, which possess different alkyl side chain lengths. We found the hydrophobicity

of these micellar core significantly affected by the different alkyl side chain. Moreover, after the encapsulation of hydrophobic doxorubicin, the drug release rate was also related to the hydrophobicity of micellar core. Although DOX-loaded micelles with the lowest hydrophobic core showed the most powerful inhibition in vitro, the increased hydrophobicity of micellar core significantly enhanced tumor growth inhibition in a MDA-MB-231 tumor model because of the prolonged circulation time, enhanced drug retention in tumors, and reduced unnecessary drug loss in tumor microenvironment. Overall, this research demonstrated the hydrophobicity of polymeric core could play a key role on the antitumor efficacy of drug delivery systems.

■ ASSOCIATED CONTENT

Supporting Information

^{1}H NMR spectrum of the micelles in D_2O, DSC traces for polymers, fluorescent spectrum of DOX-loaded micelles, body weights of mice. This material is available free of charge via the Internet at http://pubs.acs.org.

■ AUTHOR INFORMATION

Corresponding Author

*E-mail: yangxz@hfut.edu.cn.

Author Contributions

§C. Y. Sun and Y. C. Ma contributed equally to this work.

Notes

The authors declare no competing financial interest.

■ ACKNOWLEDGMENTS

This work was supported by the Ministry of Science and Technology of the People's Republic of China (2014AA020708), the National Natural Science Foundation of China (51473043, 51203145, 21304028, 51390482), the Fundamental Research Funds for the Central Universities (2014HGCH0014), and the Key Project of Anhui Provincial Educational Department (JZ2014AJZR0113). The authors also acknowledge Prof. Jun Wang (University of Science & Technology of China) for support.

■ REFERENCES

(1) Cho, K.; Wang, X.; Nie, S. M.; Chen, Z.; Shin, D. M. Therapeutic Nanoparticles for Drug Delivery in Cancer. *Clin. Cancer Res.* **2008**, *14*, 1310−1316.

(2) Brigger, I.; Dubernet, C.; Couvreur, P. Nanoparticles in Cancer Therapy and Diagnosis. *Adv. Drug Delivery Rev.* **2002**, *54*, 631−651.

(3) Hensley, M. L.; Schuchter, L. M.; Lindley, C.; Meropol, N. J.; Cohen, G. I.; Broder, G.; Gradishar, W. J.; Green, D. M.; Langdon, R. J.; Mitchell, B.; Negrin, R.; Szatrowski, T. P.; Thigpen, J. T.; Von Hoff, D.; Wasserman, T. H.; Winer, E. P.; Pfister, D. G.; Amer Soc Clinical, O. American Society of Clinical Oncology Clinical Practice Guidelines for the Use of Chemotherapy and Radiotherapy Protectants. *J. Clin. Oncol.* **1999**, *17*, 3333−3355.

(4) Shapiro, C. L.; Recht, A. Drug Therapy - Side Effects of Adjuvant Treatment of Breast Cancer. *N. Engl. J. Med.* **2001**, *344*, 1997−2008.

(5) Tang, S.; Huang, X.; Chen, X.; Zheng, N. Hollow Mesoporous Zirconia Nanocapsules for Drug Delivery. *Adv. Funct. Mater.* **2010**, *20*, 2442−2447.

(6) Jain, R. K.; Stylianopoulos, T. Delivering Nanomedicine to Solid Tumors. *Nat. Rev. Clin. Oncol.* **2010**, *7*, 653−664.

(7) Liang, Y. H.; Liu, C. H.; Liao, S. H.; Lin, Y. Y.; Tang, H. W.; Liu, S. Y.; Lai, I. R.; Wu, K. C. W. Cosynthesis, of Cargo-Loaded Hydroxyapatite/Alginate Core-Shell Nanoparticles (HAP@Alg) as pH-Responsive Nanovehicles by a Pre-gel Method. *ACS Appl. Mater. Interfaces* **2012**, *4*, 6719−6726.

(8) Fang, J.; Nakamura, H.; Maeda, H. The EPR effect: Unique Features of Tumor Blood Vessels for Drug Delivery, Factors Involved, and Limitations and Augmentation of the Effect. *Adv. Drug Delivery Rev.* **2011**, *63*, 136−151.

(9) Zhang, Z.; Chen, X. F.; Chen, L.; Yu, S. J.; Cao, Y.; He, C. L.; Chen, X. S. Intracellular pH-Sensitive PEG-block-Acetalated-Dextrans as Efficient Drug Delivery Platforms. *ACS Appl. Mater. Interfaces* **2013**, *5*, 10760−10766.

(10) Bastakoti, B. P.; Inuoe, M.; Yusa, S. I.; Liao, S. H.; Wu, K. C. W.; Nakashima, K.; Yamauchi, Y. A Block Copolymer Micelle Template for Synthesis of Hollow Calcium Phosphate Nanospheres with Excellent Biocompatibility. *Chem. Commun.* **2012**, *48*, 6532−6534.

(11) Chen, L. L.; Jiang, T.; Cai, C. H.; Wang, L. Q.; Lin, J. P.; Cao, X. G. Polypeptide-Based "Smart" Micelles for Dual-Drug Delivery: A Combination Study of Experiments and Simulations. *Adv. Healthcare Mater.* **2014**, *3*, 1508−1517.

(12) Shi, J.; Xiao, Z.; Kamaly, N.; Farokhzad, O. C. Self-Assembled Targeted Nanoparticles: Evolution of Technologies and Bench to Bedside Translation. *Acc. Chem. Res.* **2011**, *44*, 1123−1134.

(13) Tyrrell, Z. L.; Shen, Y.; Radosz, M. Fabrication of Micellar Nanoparticles for Drug Delivery through the Self-Assembly of Block Copolymers. *Prog. Polym. Sci.* **2010**, *35*, 1128−1143.

(14) Mochida, Y.; Cabral, H.; Miura, Y.; Albertini, F.; Fukushima, S.; Osada, K.; Nishiyama, N.; Kataoka, K. Bundled Assembly of Helical Nanostructures in Polymeric Micelles Loaded with Platinum Drugs Enhancing Therapeutic Efficiency against Pancreatic Tumor. *ACS Nano* **2014**, *8*, 6724−6738.

(15) Plummer, R.; Wilson, R. H.; Calvert, H.; Boddy, A. V.; Griffin, M.; Sludden, J.; Tilby, M. J.; Eatock, M.; Pearson, D. G.; Ottley, C. J.; Matsumura, Y.; Kataoka, K.; Nishiya, T. A Phase I Clinical Study of Cisplatin-Incorporated Polymeric Micelles (NC-6004) in Patients with Solid Tumours. *Br. J. Cancer* **2011**, *104*, 593−598.

(16) Duan, X. P.; Xiao, J. S.; Yin, Q.; Zhang, Z. W.; Yu, H. J.; Mao, S. R.; Li, Y. P. Smart pH-Sensitive and Temporal-Controlled Polymeric Micelles for Effective Combination Therapy of Doxorubicin and Disulfiram. *ACS Nano* **2013**, *7*, 5858−5869.

(17) Davis, M. E.; Chen, Z.; Shin, D. M. Nanoparticle Therapeutics: An Emerging Treatment Modality for Cancer. *Nat. Rev. Drug Discovery* **2008**, *7*, 771−782.

(18) Medina, S. H.; Tiruchinapally, G.; Chevliakov, M. V.; Durmaz, Y. Y.; Stender, R. N.; Ensminger, W. D.; Shewach, D. S.; ElSayed, M. E. H. Targeting Hepatic Cancer Cells with PEGylated Dendrimers Displaying N-Acetylgalactosamine and SP94 Peptide Ligands. *Adv. Healthcare Mater.* **2013**, *2*, 1337−1350.

(19) Harris, J. M.; Chess, R. B. Effect of Pegylation on Pharmaceuticals. *Nat. Rev. Drug Discovery* **2003**, *2*, 214−221.

(20) Owens, D. E.; Peppas, N. A. Opsonization, Biodistribution, and Pharmacokinetics of Polymeric Nanoparticles. *Int. J. Pharm.* **2006**, *307*, 93−102.

(21) Veronese, F. M.; Pasut, G. PEGylation, Successful Approach to Drug Delivery. *Drug Discovery Today* **2005**, *10*, 1451−1458.

(22) Li, Y.; Gao, G. H.; Lee, D. S. Stimulus-Sensitive Polymeric Nanoparticles and Their Applications as Drug and Gene Carriers. *Adv. Healthcare Mater.* **2013**, *2*, 388−417.

(23) Graf, N.; Bielenberg, D. R.; Kolishetti, N.; Muus, C.; Banyard, J.; Farokhzad, O. C.; Lippard, S. J. alpha(V)beta(3) Integrin-Targeted PLGA-PEG Nanoparticles for Enhanced Anti-tumor Efficacy of a Pt(IV) Prodrug. *ACS Nano* **2012**, *6*, 4530−4539.

(24) Zheng, M.; Yue, C.; Ma, Y.; Gong, P.; Zhao, P.; Zheng, C.; Sheng, Z.; Zhang, P.; Wang, Z.; Cai, L. Single-Step Assembly of DOX/ICG Loaded Lipid-Polymer Nanoparticles for Highly Effective Chemo-Photothermal Combination Therapy. *ACS Nano* **2013**, *7*, 2056−2067.

(25) Zhang, P. C.; Hu, L. J.; Yin, Q.; Zhang, Z. W.; Feng, L. Y.; Li, Y. P. Transferrin-Conjugated Polyphosphoester Hybrid Micelle Loading Paclitaxel for Brain-Targeting Delivery: Synthesis, Preparation and *in vivo* Evaluation. *J. Controlled Release* **2012**, *159*, 429−434.

(26) Loh, X. J.; Ong, S. J.; Tung, Y. T.; Choo, H. T. Dual Responsive Micelles Based on Poly (R)-3-Hydroxybutyrate and Poly(2-(Di-

Methylamino) Ethyl Methacrylate) for Effective Doxorubicin Delivery. *Polym. Chem.* **2013**, *4*, 2564−2574.
(27) Seyednejad, H.; Ghassemi, A. H.; van Nostrum, C. F.; Vermonden, T.; Hennink, W. E. Functional Aliphatic Polyesters for Biomedical and Pharmaceutical Applications. *J. Controlled Release* **2011**, *152*, 168−176.
(28) Feng, J.; Zhuo, R. X.; Zhang, X. Z. Construction of Functional Aliphatic Polycarbonates for Biomedical Applications. *Prog. Polym. Sci.* **2012**, *37*, 211−236.
(29) Cameron, D. J. A.; Shaver, M. P. Aliphatic Polyester Polymer Stars: Synthesis, Properties and Applications in Biomedicine and Nanotechnology. *Chem. Soc. Rev.* **2011**, *40*, 1761−1776.
(30) Hrkach, J.; Von Hoff, D.; Ali, M. M.; Andrianova, E.; Auer, J.; Campbell, T.; De Witt, D.; Figa, M.; Figueiredo, M.; Horhota, A.; Low, S.; McDonnell, K.; Peeke, E.; Retnarajan, B.; Sabnis, A.; Schnipper, E.; Song, J. J.; Song, Y. H.; Summa, J.; Tompsett, D.; Troiano, G.; Hoven, T. V. G.; Wright, J.; LoRusso, P.; Kantoff, P. W.; Bander, N. H.; Sweeney, C.; Farokhzad, O. C.; Langer, R.; Zale, S. Preclinical Development and Clinical Translation of a PSMA-Targeted Docetaxel Nanoparticle with a Differentiated Pharmacological Profile. *Sci. Transl. Med.* **2012**, *4*, 128−139.
(31) Xiao, C. S.; Wang, Y. C.; Du, J. Z.; Chen, X. S.; Wang, J. Kinetics and Mechanism of 2-ethoxy-2-oxo-1,3,2-dioxaphospholane Polymerization Initiated by Stannous Octoate. *Macromolecules* **2006**, *39*, 6825−6831.
(32) Zhang, S. Y.; Zou, J.; Zhang, F. W.; Elsabahy, M.; Felder, S. E.; Zhu, J. H.; Pochan, D. J.; Wooley, K. L. Rapid and Versatile Construction of Diverse and Functional Nanostructures Derived from a Polyphosphoester-Based Biomimetic Block Copolymer System. *J. Am. Chem. Soc.* **2012**, *134*, 18467−18474.
(33) Song, W. J.; Du, J. Z.; Liu, N. J.; Dou, S.; Cheng, J.; Wang, J. Functionalized Diblock Copolymer of Poly(epsilon-caprolactone) and Polyphosphoester Bearing Hydroxyl Pendant Groups: Synthesis, Characterization, and Self-Assembly. *Macromolecules* **2008**, *41*, 6935−6941.
(34) Du, J. Z.; Du, X. J.; Mao, C. Q.; Wang, J. Tailor-Made Dual pH-Sensitive Polymer-Doxorubicin Nanoparticles for Efficient Anticancer Drug Delivery. *J. Am. Chem. Soc.* **2011**, *133*, 17560−17563.
(35) Wang, H. X.; Xiong, M. H.; Wang, Y. C.; Zhu, J.; Wang, J. N-Acetylgalactosamine Functionalized Mixed Micellar Nanoparticles for Targeted Delivery of siRNA to Liver. *J. Controlled Release* **2013**, *166*, 106−114.
(36) Wen, J.; Zhuo, R. X. Preparation and Characterization of Poly(D,L-Lactide-co-Ethylene Methyl Phosphate). *Polym. Int.* **1998**, *47*, 503−509.
(37) Yang, X. Z.; Sun, T. M.; Dou, S.; Wu, J.; Wang, Y. C.; Wang, J. Block Copolymer of Polyphosphoester and Poly(L-Lactic Acid) Modified Surface for Enhancing Osteoblast Adhesion, Proliferation, and Function. *Biomacromolecules* **2009**, *10*, 2213−2220.
(38) Cheng, Y. L.; He, C. L.; Xiao, C. S.; Ding, J. X.; Ren, K. X.; Yu, S. J.; Zhuang, X. L.; Chen, X. S. Reduction-Responsive Cross-Linked Micelles Based on PEGylated Polypeptides Prepared via Click Chemistry. *Polym. Chem.* **2013**, *4*, 3851−3858.
(39) Clement, B.; Grignard, B.; Koole, L.; Jerome, C.; Lecomte, P. Metal-Free Strategies for the Synthesis of Functional and Well-Defined Polyphosphoesters. *Macromolecules* **2012**, *45*, 4476−4486.
(40) Gong, P.; Yang, Y. T.; Yi, H. Q.; Fang, S. T.; Zhang, P. F.; Sheng, Z. H.; Gao, G. H.; Gao, D. Y.; Cai, L. T. Polypeptide Micelles with Dual pH Activatable Dyes for Sensing Cells and Cancer Imaging. *Nanoscale* **2014**, *6*, 5416−5424.
(41) Yuan, Y. Y.; Mao, C. Q.; Du, X. J.; Du, J. Z.; Wang, F.; Wang, J. Surface Charge Switchable Nanoparticles Based on Zwitterionic Polymer for Enhanced Drug Delivery to Tumor. *Adv. Mater.* **2012**, *24*, 5476−5480.
(42) Sun, C. Y.; Dou, S.; Du, J. Z.; Yang, X. Z.; Li, Y. P.; Wang, J. Doxorubicin Conjugate of Poly(Ethylene Glycol)-Block Polyphosphoester for Cancer Therapy. *Adv. Healthcare Mater.* **2014**, *3*, 261−272.
(43) Yang, X. Z.; Dou, S.; Wang, Y. C.; Long, H. Y.; Xiong, M. H.; Mao, C. Q.; Yao, Y. D.; Wang, J. Single-Step Assembly of Cationic Lipid-Polymer Hybrid Nanoparticles for Systemic Delivery of siRNA. *ACS Nano* **2012**, *6*, 4955−4965.
(44) Ma, Y. C.; Wang, J. X.; Tao, W.; Qian, H. S.; Yang, X. Z. Polyphosphoester-Based Nanoparticles with Viscous Flow Core Enhanced Therapeutic Efficacy by Improved Intracellular Drug Release. *ACS Appl. Mater. Interfaces* **2014**, *6*, 16174−16181.
(45) Tewey, K. M.; Rowe, T. C.; Yang, L.; Halligan, B. D.; Liu, L. F. Adriamycin-Induced DNA Damage Mediated by Mammalian DNA Topoisomerase II. *Science* **1984**, *226*, 466−468.